Materialia 5 (2019) 100241

Contents lists available at ScienceDirect

Materialia

journal homepage: www.elsevier.com/locate/mtla

Full Length Article

Towards understanding the evolution of dislocation loops and their interaction with vacancies in Fe9Cr alloy during the irradiation swelling incubation period

Shuoxue Jin[a,*], Bing Mo[b], Weiping Zhang[c], Tongmin Zhang[d], Yang Li[b,*], Liping Guo[c], Xingzhong Cao[a], Baoyi Wang[a]

[a] Multi-Discipline Research Center, Institute of High Energy Physics, Chinese Academy of Sciences, Beijing 100049, China
[b] Center for Lunar and Planetary Sciences, Institute of Geochemistry, Chinese Academy of Sciences, Guiyang 550081, China
[c] Key Laboratory of Artificial Micro- and Nano-structures of Ministry of Education and School of Physics and Technology, Wuhan University, Wuhan 430072, China
[d] Institute of Modern Physics, Chinese Academy of Sciences, Lanzhou 730000, China

ARTICLE INFO

Keywords:
Dislocation loops
Vacancies
Positron annihilation spectroscopy
FeCr alloy

ABSTRACT

It is well known that body-centered cubic metals have much longer swelling incubation periods than face-centered cubic metals during neutron or charged particle irradiation. In this paper, Fe9Cr model alloy was irradiated with 2 MeV self-ions to lower doses of 0.5, 1.0 and 3.0 dpa at room temperature. The evolution of microstructural defects was revealed by transmission electron microscopy and positron annihilation spectroscopy. Small interstitial dislocation loops were observed in the form of black spots and they were accompanied by a large number of vacancies after 0.5 dpa. Visible dislocation loops dominated the microstructure after irradiation with 1.0 dpa and 3.0 dpa, but the sharp decrement of the S value means that the vacancies should be annihilated gradually with the irradiation dose increasing. In addition, the vacancy status was further confirmed by the investigation of their occupation behaviors with low-energy deuterium atoms. The vacancies located around loops would be trapped and removed by the coarsening interstitial dislocation loops. We believe that the understanding of the interaction between vacancies and dislocation loops is a possible complementary mechanism, applicable for explaining the long stage of swelling incubation in bcc metals.

1. Introduction

It is well known that a high void swelling rate and levels are no doubt detrimental to mechanical properties such as irradiation creep and embrittlement for austenitic stainless steels, with the consequences of limiting their further use in advanced nuclear reactor concepts [1]. Garner et al. have compared swelling behavior of body-centered cubic (bcc) ferritic/martensitic (F/M) alloys and face-centered cubic (fcc) during high neutron irradiation [2]. Simple fcc metals have a very short incubation period and steady-state swelling rate of ~1%/dpa, whereas simple bcc metals exhibit a lower steady-state swelling rate (~0.2%/dpa) after longer swelling incubation periods [2–5]. Ferritic and F/M steels swell much less than austenitic stainless steels during neutron or charged particle irradiation. As a result, the development efforts for F/M steels in advanced nuclear reactor concepts have been paid more attention than austenitic alloys.

F/M steels have been identified as are one of the candidate core structural materials for Generation IV fission reactors and high-power accelerator spallation targets [6–8]. Furthermore, reduced activation ferritic/martensitic (RAFM) steels are the prime choice for the structural material of the first wall in the fusion reactors [9–11]. F/M steels such as T91 [12], P92 [13], 9Cr2WVTa [8], Eurofer97 [7], JLF-1 [14], CLAM [15,16], and SCRAM [17] steels are based on Fe9Cr, and a handful of studies employing neutron or charged particle have shown the above Fe9Cr based on F/M steel possess excellent resistance to irradiation swelling [7–9,11–17].

It is well known that the origin and growth of void swelling is due to excess vacancies left in matrix while the interstitial atoms move to the surface quickly [18]. During the swelling incubation period, dislocation or dislocation loops were observed prior to the onset of steady-state swelling, whether in bcc steels (such as FeCr binary alloys [11,19]) or in fcc steels (such as SUS316SS [20]). The dislocation or dislocation loops not only absorb the interstitial atoms over vacancies owing to their dislocation bias, but also promote the interstitial atoms to the surface, acting as a pathway. The vacancies were left behind, which is smaller than the resolution limit of transmission electron microscopy (TEM) during

* Corresponding authors.
E-mail addresses: jinshuoxue@ihep.ac.cn (S. Jin), liyang@mail.gyig.ac.cn (Y. Li).

https://doi.org/10.1016/j.mtla.2019.100241
Received 27 November 2018; Accepted 31 January 2019
Available online 4 February 2019

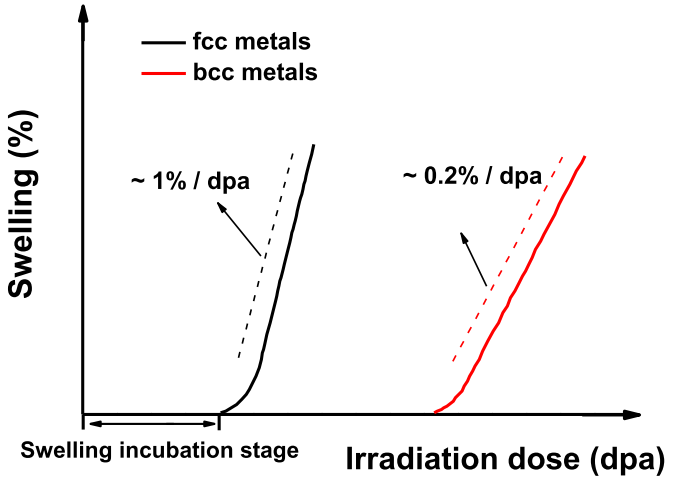

Fig. 1. Illustration of comparison shows that the swelling incubation stage is longer for bcc metals than fcc metals.

swelling incubation period. Therefore, the evolution of the leaving vacancies during the swelling incubation period and their interaction with dislocation loops under increased irradiation dose, are difficult and essential to understand mechanisms of the longer incubation time in the bcc metals.

Positron annihilation technique is a very sensitive tool for detecting vacancy-type defects in materials. TEM used to characterize the nature and Burgers vector of dislocation loops and their evolution under increased irradiation dose. In the present paper, we attempt to study the evolution of dislocation loops and their interaction with vacancies in Fe9Cr alloy in the stage of swelling incubation. In addition, the vacancy status was also confirmed further by investigating occupation behaviors with deuterium atoms.

2. Experimental details

In the present work, Fe9Cr binary model alloy was melted from high purity Fe (99.99%) and Cr (99.99%) metals in a vacuum argon arc furnace located at General Research Institute for Nonferrous Metals. The bulk material was first cut into $10\times10\times1\ mm^3$ square sheets by wire electrical discharge machining, and then mechanically and electrochemically polished ($75\%CH_3COOH+25\%HClO_4$, at ~10 °C) to a mirror-like surface. Subsequently, the polished sheet specimens were well-annealed at 1100 K for 2 h in vacuum ($\sim10^{-5}$ Pa).

As we known that the swelling incubation stage is much longer for bcc metals than fcc metals prior to the onset of steady-state swelling as illustrated in Fig. 1. Vacancies and dislocation loops were first introduced into the well-annealed specimens by irradiation with 2 MeV self (Fe^{13+}) ion. The highest irradiation dose is 3 dpa, which is far behind the dose levels that swelling occurred (>10 dpa) in FeCr binary model alloys [3]. The irradiation experiments were carried out at the 320 kV platform for multi-discipline research with highly charged ions at the Institute of Modern Physics. The uniform ion beam (~820 nA) was obtained by scanning along the X and Y directions. The specimens were irradiated at room temperature to the fluences of $0.23\times10^{15}/cm^2$, $0.45\times10^{15}/cm^2$ and $1.4\times10^{15}/cm^2$, corresponding to the peak doses of 0.5 dpa 1.0 dpa and 3.0 dpa, respectively. The 2 MeV Fe^{13+} irradiation profiles, i.e., $1.4\times10^{15}/cm^2$ (~3.0 peak dpa), were simulated by SRIM, as shown in Fig. 2, and the displacement energy E_d was set as 40 eV. The heavy ion irradiation defects were first identified by a JEM-2010HT TEM located at Wuhan University. The cross-sectional TEM specimens were prepared by the focused ion beam (FIB) system (FEI Scios) at Institute of Geochemistry, as well as low energy (2 keV) Ga ion milling with an incident angle of 7° was performed to remove the damage region by high energy Ga ions.

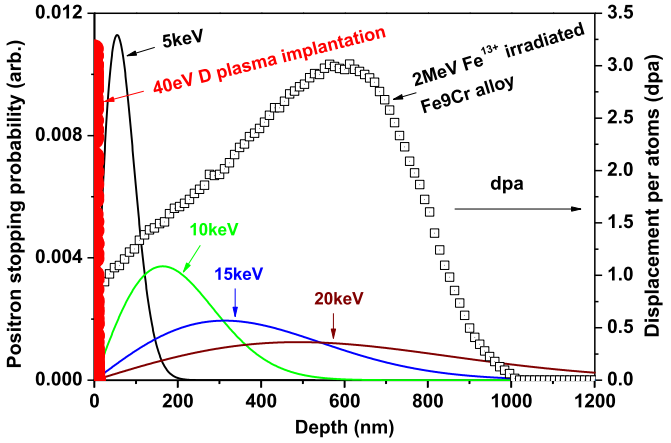

Fig. 2. Depth profiles of the calculated positron penetration and the displacement damage in Fe9Cr alloy. The positron implantation energies were 5 keV, 10 keV, 15 keV and 20 keV, respectively, and the Fe9Cr alloy was irradiated by 2 MeV Fe^{13+} to a dose of $1.4\times10^{15}/cm^2$ (~3.0 peak dpa). Subsequently, all the Fe^{13+} irradiated specimens were exposed to deuterium plasma to a fluence of $1\times10^{21}\ D^+/cm^2$.

Subsequently, all the damaged sheet Fe9Cr specimens were exposed to low energy deuterium plasma at ~100 °C in a linear plasma device named STEP (simulator for tokamak edge plasma) at Beihang University [21]. The implanted energy is ~40 eV and the fluence is about $1\times10^{21}/cm^2$. Fig. 2 also shows that the low (~40 eV) energy (equal to the displacement threshold) deuterium ions cannot produce the vacancies in Fe9Cr alloy. They gathered in the surface region due to the shorter implantation range (<10 nm), but they could diffusion into the interior of alloy. The evolution of microstructural defects induced by self-ion irradiation and their capturing deuterium behaviors were investigated by positron annihilation Doppler broadening spectroscopy using a slow positron beam facility in Institute High Energy Physics. The S parameter, which represents the information annihilated with low momentum electron, is defined as the ratio of the central area (510.2–511.8 keV) to the total region (499.5–522.5 keV), while the W parameter is the ratios of two flanks high momentum regions (505.1–508.4 keV and 513.6–516.9 keV) to the total region. The positron penetration distribution $P(x,E)$ in the materials could be taken as the Makhovian profile [22,23]:

$$P(x,\ E)=-\frac{d}{dx}\left\{\exp\left[-\left(\frac{x}{x_0}\right)^m\right]\right\} \tag{1}$$

where

$$x_0=\frac{\bar{x}}{\Gamma\left[\left(\frac{1}{m}\right)+1\right]} \tag{2}$$

where m=2 is empirical parameter, $\bar{x}$ denotes the mean detecting depth of the positrons, which varies with the implantation positron energy E (in keV):

$$\bar{x}(E)=\frac{\alpha}{\rho}E^n \tag{3}$$

where $\alpha=4\times10^{-5}\ kg/m^2\ keV^{1.6}$, n=1.6, according to the empirical parameters [24], ρ is the sample density (in kg/m^3, $7.801\times10^3 kg/m^3$ for the Fe9Cr alloy), and Γ is the gamma function. Thus, the calculated positron penetration profiles $P(x,E)$ for the four implantation energies (5 keV, 10 keV, 15 keV and 20 keV) are also shown in Fig. 2.

3. Results and discussion

Fig. 3 shows the microstructural evolution of Fe9Cr irradiated at room temperature with 2 MeV self-ions to doses of 0, 0.5, 1.0 and 3.0 dpa. In Fig. 3a, an unirradiated specimen, exhibiting a defect-free

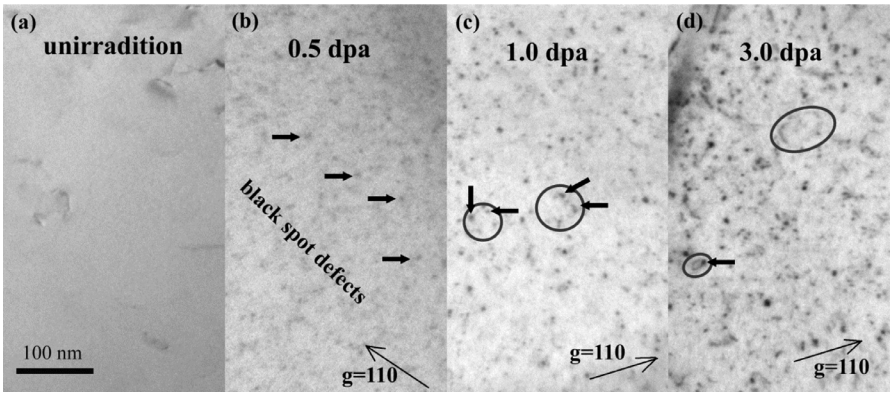

Fig. 3. Development of damage structures in Fe9Cr alloy irradiated with 2 MeV self-ions to doses of 0 dpa (a), 0.5 dpa (b), 1.0 dpa (c), and 3.0 dpa (d). For these measurements, weak beam bright field images were imaged by using $\boldsymbol{g}=110$ near the [001] zone axis.

micrograph, represents that it was well annealed after 1100 K for 2 h. All the irradiated specimens were normally imaged near the [001] zone axis orientation (Fig. 3b and c). In the weak beam bright field image $\boldsymbol{g}(3\boldsymbol{g})$=110, small "black spot" defect clusters are formed after the irradiation. A major part of small black spot defects ranged of 2–5 nm (see the arrows) homogeneously distributed in the matrix of the steel, as shown in Fig. 3b. With respect to the black spot defects, in fact, it is very difficult to identify whether they are point defect clusters or dislocation loops. Dislocation loops result from "discs collapse" caused by theirs instability as the disc size attains tens of point defect clusters (vacancies or interstitials) [25,26]. Most of the previous experiments have achieved a general consensus that 1/2<111> and ⟨100⟩ interstitial loops are formed in iron, ferritic steels, and bcc materials after irradiation, according to the $\boldsymbol{g}\cdot\boldsymbol{b}=0$ invisibility criterion [11,27–29]. The classical dislocation bias physically underlines the preference of absorption of interstitial atoms over vacancies by dislocation lines [30]. Both the 1/2<111> and ⟨100⟩ interstitial loops would constantly absorb the interstitial atoms and the disc collapse region would coarsen. By a dose of 1.0 dpa, the damage of the structure has developed further, i.e., the visible dislocation loops marked by black rings have formed in Fig. 3c. It should be noted that small black spot defects (indicated by the arrows) were frequently seen decorating the larger visible loops. The loops were possibly enhanced by the absorption of black spot defects. The density of the dislocation loop increased following the 3.0 dpa irradiation (Fig. 3d). Meanwhile, many small black spots lie on the line of the dislocation loops, and the line-width of the dislocation loops increased. This means that the visible dislocation loops dominated the microstructure after irradiation with 1.0 dpa and 3.0 dpa.

Fig. 4 shows the dependence of S parameters on the positron energy (mean detecting depth) for Fe9Cr alloy irradiated with different doses. The mean detecting depths were calculated and shown in the upper horizontal scale of Fig. 4 according to Eq. (3). The S value in the 0.5-dpa-irradiated specimen increased obviously compared with the unirradiated one. However, the S value decreased instead when the irradiation dose increased to 1.0 dpa and 3.0 dpa. It is well known that the positron is very sensitive to the vacancy-type clusters. The sharp decrement in the S value means that the vacancies should be removed and annihilated gradually by increasing the irradiation dose. It is an unexpected and abnormal phenomenon for the evolution of the vacancy-type clusters, and it is different from our previous work. The S values in the FeCu [31,32] and FeCrNi [33] alloys would increase or reach a saturation value with the increasing irradiation dose.

Compared with the TEM results in Fig. 3, many black spot defects are formed after 0.5 dpa irradiation; visible dislocation loops appeared and their density increased as the irradiation dose increased to 1.0 dpa and 3.0 dpa. In the initial irradiation stage, the interstitial atoms gather into disks prior to the vacancies because of their lower migration energy, which collapse to form an interstitial dislocation loop. The black spot defects in Fig. 3a should be mainly interstitial dislocation loops.

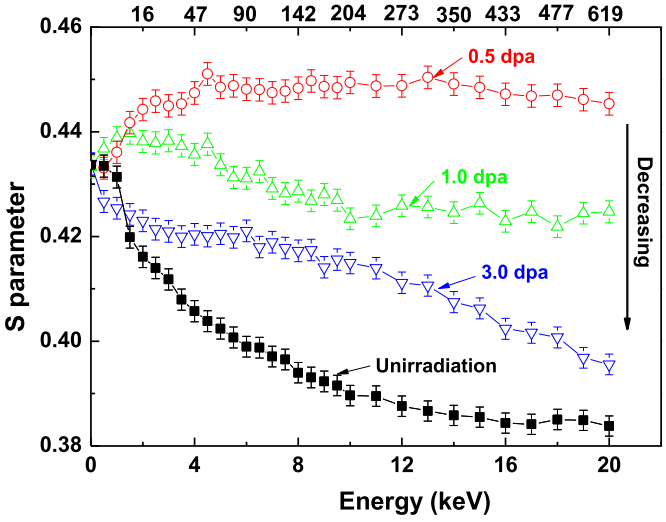

Fig. 4. Evolution of the S–E curves in Fe9Cr specimens irradiated with self-ions to doses of 0 dpa, 0.5 dpa, 1.0 dpa and 3.0 dpa.

According to the classical dislocation bias theory, the dislocation loops should prefer to absorb the interstitial atoms [30,34]. The vacancies remain in the matrix and enhance the S value in a 0.5-dpa-irradiated specimen. However, with the formation and increment of visible dislocation loops, how do they affect the evolution of the vacancies? What is the mechanism for the vacancies and dislocation loops? Given that there are different defect types, the S value represents the different positron affinities. The positron affinity has been calculated and summarized for a vacancy, dislocation line, and a vacancy on a dislocation line in Fe by Kuramoto et al., which gave the positron lifetime as 175 ps for a single vacancy in matrix, 117 ps for an edge dislocation, and 140 ps for a single vacancy on an edge dislocation [35,36]. A lower positron affinity is observed for dislocation loops than vacancy-type defects (such as vacancies and voids). The positron annihilation lifetime in the matrix for pure Fe is 110 ps. Therefore, the S parameter is mainly determined by the type of vacancy-type clusters but not by the dislocation loop, and the positron affinity of the dislocation loop is similar to that of the matrix. Thus, we propose a simple possibility that size coarsening of loops would close to the surrounding vacancies and reduce their movability and aggregation, or even absorb and annihilate them.

Fig. 5 shows the S-W plot for Fe9Cr samples irradiated with different doses, which represents the annihilation mechanism for different defects. Most of the (S, W) points lied on line L_1 correspond to the unirradiated specimen/bulk state, which suggests that most of the positrons annihilate with Fe electrons (free electrons). In contrast, more complicated S-W interaction took place for all the irradiation specimens, and

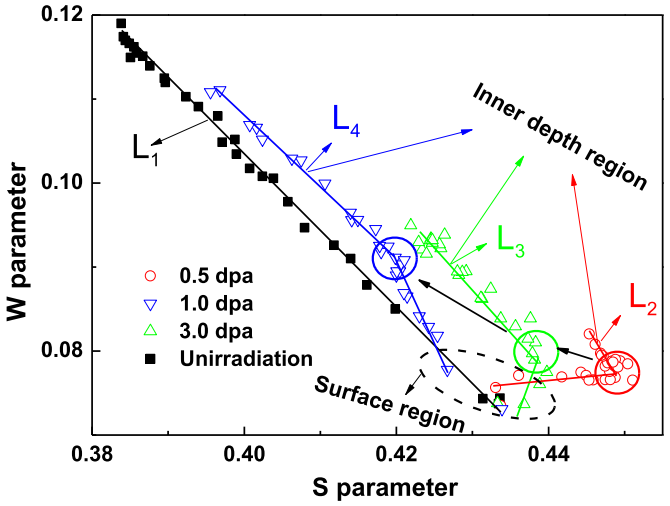

Fig. 5. S-W relation for Fe9Cr samples irradiated with doses of 0.5 dpa, 1.0 dpa and 3.0 dpa. The unirradiated specimen shown here as a reference represents positron annihilation mechanism with free electron of the matrix.

the slope changing points marked by colored circles were observed in the S-W plot. Neglecting the (S, W) points in the surface region, more than half of the (S, W) points for the 0.5-irradiated-specimens are on the slope changing point region marked by the red circle, and a few of the points lie on L_2. These suggest small interstitial dislocation loops have been formed, and they were accompanied by many vacancies. With the irradiation dose increases, and the slope changing point region moves to the bulk state as indicated by the arrows. Meanwhile, the slope value decreases gradually with increasing irradiation dose ($L_4 < L_3 < L_2$), and more and more (S, W) points lie on L_3 and L_4. In particular, the slope of L_4 was almost the same with the bulk state (L_1). These mean that coarsening of the interstitial dislocation loops could then occur by constantly absorbing interstitial atoms and coalescing the smaller loops directly.

Vacancies cannot be observed by TEM as shown in Fig. 3 due to inadequate resolution. Low-energy deuterium ions were introduced into the self-ion damaged Fe9Cr specimens. Deuterium atoms diffused freely until they were trapped by the defects matrix, and no secondary vacancy defects were produced during the process of low-energy deuterium ion implantation. Investigation of occupation behaviors of vacancies with deuterium atoms could deduce indirectly the vacancy status at different irradiation doses. Certainly, once they encounter dislocation loops, pipe-diffusion of deuterium atoms along the dislocation lines may also lead to a transfer of the matter around the loops [37–39], and the diffusion rate would be enhanced. As we know, the ability to capture gas atoms is stronger for vacancies than interstitial dislocation loops; we mainly focus the occupation behaviors of vacancies with deuterium atoms and do not consider the pipe-diffusion of deuterium atoms in the present article. Our previous study indicated that hydrogen atoms occupied vacancy sites and V_mH_n complexes were formed, and they can affect the annihilation of positrons with electrons in the vacancy defects [40]. Xu et al. also showed that deuterium were trapped by vacancies induced by Cu ion irradiation, which resulted in a decrease in S parameters [41]. Vacancies and voids can reduce the electron density in their vicinity to provide a trapping site for hydrogen isotope embedding [42,43]. Eventually, when hydrogen isotope atoms embedded in a vacancy, incrementing electron density will reduce the positron affinity for vacancies. Fig. 6a shows the changes of S parameters for self-ion damaged Fe9Cr specimens exposed to 40 eV deuterium ions, and the same fluence ($\sim 1\times10^{21}/cm^2$) deuterium atoms were introduced into different specimens. Compared to the self-ion damaged specimens, all the S values except for the surface region (<1.5 keV, 0–10 nm, see rectangle in Fig. 6a) decreased after deuterium ion implantation. Therefore, deuterium atoms and vacancies are strongly attractive in metals, which is consistent with previous studies.

In order to accurately express the concentration of vacancy defects, the relative S parameters (ΔS) were denoted and shown in Fig. 6b by this calculation, i.e., $\Delta S = S - S_{unirradiation}$. In the range of 0–10 nm, corresponding to the deuterium ion implantation range according to Fig. 2, the ΔS parameters after deuterium plasma explosion have higher values than those of self-ion damaged ones. The implication is that supersaturation of deuterium atoms, similar to He [44], could be captured by vacancies induced by self-ion irradiation, and deuterium overpressurized clusters can mutate into di-vacancies by emitting an isolated self-interstitial atom and achieve an equilibrium deuterium-to-vacancy ratio. This is called a “trap mutation process”, which could enhance the S values with the existence of D supersaturation in the surface region.

In the diffusion region of deuterium atoms (>10 nm), the ΔS parameter for the 0.5 dpa + D specimen is larger than that for 1.0 dpa + D and 3.0 dpa + D specimens. It is interesting that the ΔS parameter for the 3 dpa + D specimen is slightly larger than that for 1.0 dpa + D in the range of 11–20 keV. Even, in the range of 18–20 keV, the ΔS parameter for the 3 dpa + D specimen is larger than that for 3 dpa irradiated

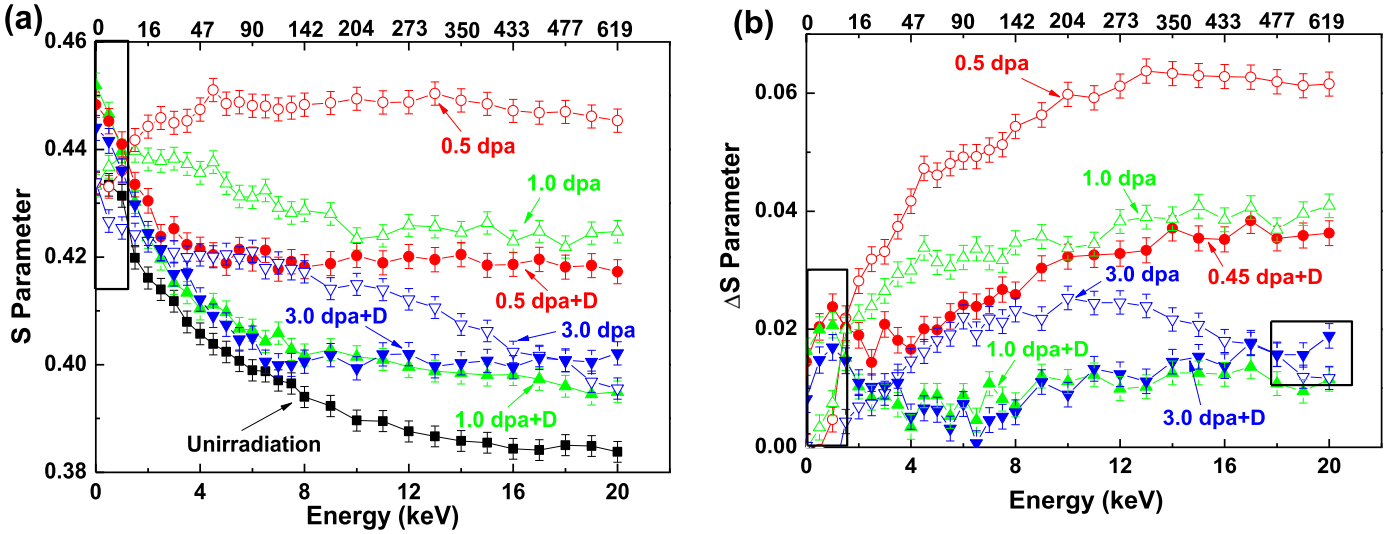

Fig. 6. (a) Absolute S parameters versus positron energy (depth) for Fe9Cr alloy irradiated with different irradiation doses. (b) Relative S parameters (ΔS) as a function of the depth. Versus depth in the top X-axis is calculated from the positron energy.

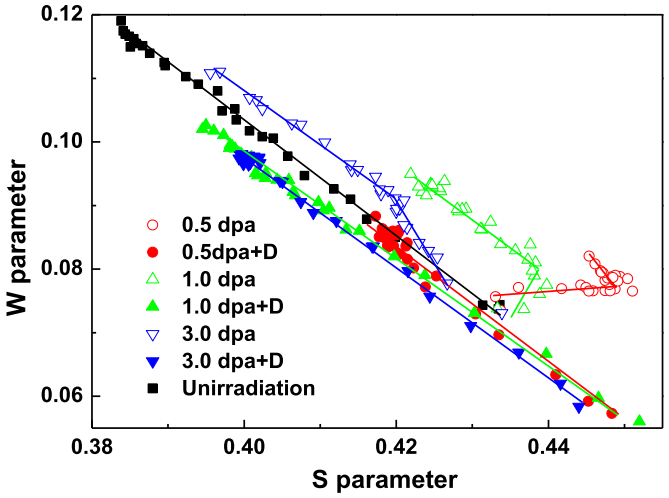

Fig. 7. S-W correlation diagram before and after deuterium ion implantation.

one, as indicated by rectangle in Fig. 6b. Liu et al. reported the vacancy trapping H mechanism in bcc metal based on first principles calculations [43]. They found that vacancy can provide 6 minimum-energy H binding sites in its vicinity due to the lower charge density. This means that the vacancy, as a trapping center, could provide an optimal isosurface of charge density (~0.11 e/Å) near the center for collecting H atoms and V_mH_n ($1 \leqslant n/m \leqslant 6$) maybe more stable complexes. The mechanism may also be suitable for deuterium atoms in the present study. However, once the deuterium atoms exceed the critical charge density, the "trap mutation process" would take place and instead mutation vacancies forms. The slight enhancement of ΔS for the 3 dpa + D specimen compared to 1.0 dpa + D is caused by excessive deuterium atoms. Fig. 7 shows the comparison for S-W correlation in Fe9Cr alloy before and after deuterium ion explosion. Compared to the S-W relation after self-ion irradiation in Fig. 5, all the (S, W) points for deuterium ion implantation specimens were almost aligned on the lines and their gradient values are almost the same as that of the unirradiated specimen, with the implication that mechanism of positron annihilation for deuterium ion implantation specimens is similar to the unirradiated one. The electron density in a vacancy's vicinity increased due to occupation with deuterium atoms. The range of (S, W) points in Fig. 7 could reflect the deuterium saturation degree in vacancies in different samples. The concentration of deuterium atoms in the 0.5 dpa + D specimen is not saturated. Therefore, introduction of low-energy deuterium atoms into the pre-damaged alloys and investigation of their occupation behaviors of vacancies by deuterium atoms could be beneficial to confirm further the vacancy status at different self-ion irradiation doses.

Depending on the results of TEM and positron annihilation spectroscopy, we offer some hypothesis for the evolution of dislocation loops and the interaction between the vacancies and interstitial dislocation loops in Fe9Cr alloy during the irradiation swelling incubation period (see Fig. 8). In the initial irradiated stage, a collision cascade produces vacancies and interstitial atoms in equal numbers. Interstitial atoms gather into unstable disks, and then collapse to loops that appear as black spots (Fig. 3b). Vacancy migration is even slower and they remain and distribute in the matrix, which increased the S value in the 0.5-dpa-irradiated specimen. As the irradiation dose increased to 1.0 dpa and 3.0 dpa, visible interstitial dislocation loops dominated the microstructure, as shown in Figs. 3c and 3d, which coarsened by constantly absorbing interstitial atoms and coalescing the smaller loops directly. Meanwhile, a sharp decrement in the S parameters with the increasing of the dislocation loops indicates that there may be an interaction between vacancies and interstitial dislocation loops. In Fig. 8, we deduce a possible understanding that the vacancies located around the loops would be trapped and removed by coarsening the interstitial dislocation loops, or vacancies migrate towards loops and annihilate there. This not only suppresses the coarsening of visible interstitial dislocation loops but also eliminate some of the vacancies. The hypothesis could be supported by previous theoretical calculated work by Chang et al. [30]. Screw dislocations have negative bias, which implies a more efficient absorption of vacancies than interstitial atoms. The repulsion zones around the dislocation drive away interstitial atoms but not vacancies.

Furthermore, the vacancy status has a large effect on the irradiation swelling phenomenon. The decrement in vacancy concentration and interaction of vacancies with dislocation loops at lower irradiation dose could delay and suppress the swelling behavior in Fe-based ferric steels. This may be an explanation why bcc metals have a long swelling incubation time.

4. Conclusion

In the present work, the Fe9Cr model alloy was irradiated with 2 MeV self-ions to lower doses of 0.5, 1.0 and 3.0 dpa at room temperature. Using the TEM and positron annihilation, we focused on the evolution of the dislocation loops and their interaction with vacancies during the irradiation swelling incubation period. In order to further gain vacancy status at different self-ion irradiation doses, low-energy deuterium atoms occupied the vacancy sites. We can know the vacancy concentration in the 0.5 dpa + D specimen is largest among the three self-ion irradiation doses by comparing the D saturation degree in the vacancies.

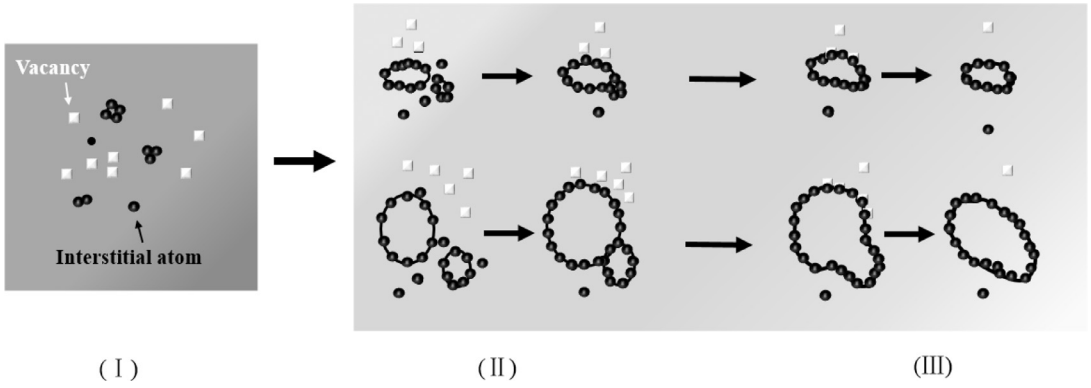

Fig. 8. Schematic of evolution of dislocation loops and their interaction with vacancies: (I) in initial irradiated stage, interstitial atoms gather into disks and collapse to form interstitial dislocation loops; (II) interstitial dislocation loops coarsened by constantly absorbing interstitial atoms and coalesce the smaller loops directly, and they would gradually close to the surrounding vacancies or vacancies migrate towards loops in the growth process; (III) when interstitial dislocation loops encounter vacancies, they would annihilate/remove them.

Small interstitial dislocation loops were observed in the form of black spots after 0.5 dpa. They would coarsen by constantly absorbing the interstitial atoms and coalescing the smaller loops directly, and visible dislocation loops dominated the microstructure after irradiation with 1.0 dpa and 3.0 dpa. However, the S value decreased sharply as the irradiation dose increased, which indicates that the vacancies should be annihilated gradually by the visible dislocation loops. Therefore, we deduce a possible understanding that the vacancies encounter interstitial dislocation loops and annihilate/remove there. The present study advances towards understanding the interaction between vacancies and dislocation loops, and is a possible complementary mechanism for explaining the longer stage of swelling incubation in bcc metals than fcc metals.

Declaration of interests

The authors declare that they have no known competing financial interests or personal relationships that could have appeared to influence the work reported in this paper.

Acknowledgments

This work is supported by the National Natural Science Foundation of China (11775236, 11505192, U1732265 and U1532134).

References

[1] J.G. Gigax, H. Kim, T.Y. Chen, F.A. Garner, L. Shao, Radiation instability of equal channel angular extruded T91 at ultra-high damage levels, Acta Mater. 132 (2017) 395–404.
[2] F.A. Garner, M.B. Toloczko, B.H. Sencer, Comparison of swelling and irradiation creep behavior of fcc-austenitic and bcc-ferritic/martensitic alloys at high neutron exposure, J. Nucl. Mater. 276 (2000) 123–142.
[3] B.H. Sencer, F.A. Garner, Compositional and temperature dependence of void swelling in model Fe-Cr base alloys irradiated in the EBR-II fast reactor, J. Nucl. Mater. 283 (2000) 164–168.
[4] M.B. Toloczko, F.A. Garner, C.R. Eiholzer, Irradiation creep and swelling of the US fusion heats of Ht9-1mo and 9cr-1mo to 208-dpa at similar-to-400-degrees-C, J. Nucl. Mater. 212 (1994) 604–607.
[5] J.G. Gigax, T. Chen, H. Kim, J. Wang, L.M. Price, E. Aydogan, S.A. Maloy, D.K. Schreiber, M.B. Toloczko, F.A. Garner, L. Shao, Radiation response of alloy T91 at damage levels up to 1000 peak dpa, J. Nucl. Mater. 482 (2016) 257–265.
[6] L.K. Mansur, A.F. Rowcliffe, R.K. Nanstad, S.J. Zinkle, W.R. Corwin, R.E. Stoller, Materials needs for fusion, generation IV fission reactors and spallation neutron sources – similarities and differences, J. Nucl. Mater. 329 (2004) 166–172.
[7] P. Jung, C. Liu, J. Chen, Retention of implanted hydrogen and helium in martensitic stainless steels and their effects on mechanical properties, J. Nucl. Mater. 296 (2001) 165–173.
[8] Y. Dai, D. Gavillet, R. Restani, Stressed capsules of austenitic and martensitic steels irradiated in SINQ target-4 in contact with liquid lead-bismuth eutectic, J. Nucl. Mater. 377 (2008) 225–231.
[9] O.V. Ogorodnikova, Z. Zhou, K. Sugiyama, M. Balden, Y. Gasparyan, V. Efimov, Surface modification and deuterium retention in reduced-activation steels under low-energy deuterium plasma exposure. Part I: undamaged steels, Nucl. Fusion 57 (2017) 036010.
[10] M. Balden, S. Elgeti, M. Zibrov, K. Bystrov, T.W. Morgan, Effect of the surface temperature on surface morphology, deuterium retention and erosion of EUROFER steel exposed to low-energy, high-flux deuterium plasma, Nucl. Mater. Energy 12 (2017) 289–296.
[11] S. Xu, Z. Yao, M.L. Jenkins, TEM characterisation of heavy-ion irradiation damage in FeCr alloys, J. Nucl. Mater. 386-88 (2009) 161–164.
[12] P. Ampornrat, G.S. Was, Oxidation of ferritic-martensitic alloys T91, HCM12A and HT-9 in supercritical water, J. Nucl. Mater. 371 (2007) 1–17.
[13] S.X. Jin, L.P. Guo, T.C. Li, J.H. Chen, Z. Yang, F.F. Luo, R. Tang, Y.X. Qiao, F.H. Liu, Microstructural evolution of P92 ferritic/martensitic steel under Ar+ ion irradiation at elevated temperature, Mater. Charact. 68 (2012) 63–70.
[14] H. Ogiwara, A. Kohyama, H. Tanigawa, H. Sakasegawa, Irradiation-induced hardening mechanism of ion irradiated JLF-1 to high fluences, Fusion Eng. Des. 81 (2006) 1091–1097.
[15] J.N. Yu, Q.Y. Huang, F.R. Wan, Research and development on the China low activation martensitic steel (CLAM), J. Nucl. Mater. 367 (2007) 97–101.
[16] Q.Y. Huang, Status and improvement of CLAM for nuclear application, Nucl. Fusion 57 (2017) 086042.
[17] X.S. Xiong, F. Yang, X.R. Zou, J.P. Suo, Effect of twice quenching and tempering on the mechanical properties and microstructures of SCRAM steel for fusion application, J. Nucl. Mater. 430 (2012) 114–118.
[18] G. Ackland, Controlling radiation damage, Science 327 (2010) 1587–1588.
[19] P.P. Liu, J.W. Bai, D. Ke, F.R. Wan, Y.B. Wang, Y.M. Wang, S. Ohnuki, Q. Zhan, Effects of deuterium implantation and subsequent electron irradiation on the microstructure of Fe-10Cr model alloy, J. Nucl. Mater. 423 (2012) 47–52.
[20] M. Horiki, T. Yoshiie, K. Sato, Q. Xu, Point defect processes in neutron irradiated Ni, Fe-15Cr-16Ni and Ti-added modified SUS316SS, Philos. Mag. 93 (2013) 1701–1714.
[21] G.H. Lu, L. Cheng, K. Arshad, Y. Yuan, J. Wang, S.Y. Qin, Y. Zhang, K.G. Zhu, G.N. Luo, H.S. Zhou, B. Li, J.F. Wu, B. Wang, Development and optimization of STEP – a linear plasma device for plasma-material interaction studies, Fusion Sci. Technol. 71 (2017) 177–186.
[22] A. Vehanen, K. Saarinen, P. Hautojarvi, H. Huomo, Profiling multilayer structures with monoenergetic positrons, Phys. Rev. B 35 (1987) 4606–4610.
[23] S.J. Huang, Z.W. Pan, J.D. Liu, R.D. Han, B.J. Ye, Simulation of positron backscattering and implantation profiles using Geant4 code, Chin. Phys. B 24 (2015) 107803.
[24] P. Parente, T. Leguey, V. de Castro, T. Gigl, M. Reiner, C. Hugenschmidt, R. Pareja, Characterization of ion-irradiated ODS Fe-Cr alloys by doppler broadening spectroscopy using a positron beam, J. Nucl. Mater. 464 (2015) 140–146.
[25] L.W. Yin, M.S. Li, Z.D. Zou, Z.G. Gong, Z.Y. Hao, Prismatic dislocation loops and concentric dislocation loops in HPHT-grown diamond single crystals, Mater. Sci. Eng. A 343 (2003) 158–162.
[26] B. Bako, E. Clouet, L.M. Dupuy, M. Bletry, Dislocation dynamics simulations with climb: kinetics of dislocation loop coarsening controlled by bulk diffusion, Philos. Mag. 91 (2011) 3173–3191.
[27] M. Klimenkov, E. Materna-Morris, A. Moslang, Characterization of radiation induced defects in EUROFER 97 after neutron irradiation, J. Nucl. Mater. 417 (2011) 124–126.
[28] J. Gao, L.J. Cui, F.R. Wan, Characterization of microstructure in hydrogen ion irradiated vanadium at room temperature and the microstructural evolution during post-irradiation annealing, Mater. Charact. 111 (2016) 1–7.
[29] Z. Yao, M. Hernandez-Mayoral, M.L. Jenkins, M.A. Kirk, Heavy-ion irradiations of Fe and Fe-Cr model alloys. Part 1: damage evolution in thin-foils at lower doses, Philos. Mag. 88 (2008) 2851–2880.
[30] Z.W. Chang, D. Terentyev, N. Sandberg, K. Samuelsson, P. Olsson, Anomalous bias factors of dislocations in bcc iron, J. Nucl. Mater. 461 (2015) 221–229.
[31] S.X. Jin, P. Zhang, E.Y. Lu, L.P. Guo, B.Y. Wang, X.Z. Cao, Correlation between Cu precipitates and irradiation defects in Fe-Cu model alloys investigated by positron annihilation spectroscopy, Acta Mater. 103 (2016) 658–664.
[32] S.X. Jin, X.Y. Lian, T. Zhu, Y.H. Gong, P. Zhang, X.Z. Cao, R.S. Yu, B.Y. Wang, Irradiation evolution of Cu precipitates in Fe1.0Cu alloy studied by positron annihilation spectroscopy, J. Nucl. Mater. 499 (2018) 65–70.
[33] E.Y. Lu, X.Z. Cao, S.X. Jin, P. Zhang, C.X. Zhang, J. Yang, Y.R. Wu, L.P. Guo, B.Y. Wang, Investigation of vacancy-type defects in helium irradiated FeCrNi alloy by slow positron beam, J. Nucl. Mater. 458 (2015) 240–244.
[34] G.W. Greenwood, A.J.E. Foreman, D.E. Rimmer, The role of vacancies and dislocations in the nucleation and growth of gas bubbles in irradiated fissile material, J. Nucl. Mater. 1 (1959) 305–324.
[35] E. Kuramoto, T. Tsutsumi, K. Ueno, M. Ohmura, Y. Kamimura, Positron lifetime calculations on vacancy clusters and dislocations in Ni and Fe, Comp. Mater. Sci. 14 (1999) 28–35.
[36] E. Kuramoto, H. Abe, M. Takenaka, F. Hori, Y. Kamimura, M. Kimura, K. Ueno, Positron annihilation lifetime study of irradiated and deformed Fe and Ni, J. Nucl. Mater. 239 (1996) 54–60.
[37] Y.X. Wang, Q. Xu, T. Yoshiie, Z.Y. Pan, Effects of edge dislocations on interstitial helium and helium cluster behavior in alpha-Fe, J. Nucl. Mater. 376 (2008) 133–138.
[38] K. Sato, T. Yoshiie, T. Ishizaki, Q. Xu, Behavior of vacancies near edge dislocations in Ni and alpha-Fe: positron annihilation experiments and rate theory calculations, Phys. Rev. B 75 (2007) 094109.
[39] Y.H. Gong, S.X. Jin, T. Zhu, L. Cheng, X.Z. Cao, L. You, G.H. Lu, L.P. Guo, B.Y. Wang, Helium self-trapping and diffusion behaviors in deformed 316L stainless steel exposed to high flux and low energy helium plasma, Nucl. Fusion 58 (2018) 046011.
[40] P. Zhang, S.X. Jin, E.Y. Lu, B.Y. Wang, Y.N. Zheng, D.Q. Yuan, X.Z. Cao, Effect of annealing on VmHn complexes in hydrogen ion irradiated Fe and Fe-0.3%Cu alloys, J. Nucl. Mater. 459 (2015) 301–305.
[41] Q. Xu, K. Sato, X.Z. Cao, P. Zhang, B.Y. Wang, T. Yoshiie, H. Watanabe, N. Yoshida, Interaction of deuterium with vacancies induced by ion irradiation in W, Nucl. Instrum. Methods B 315 (2013) 146–148.
[42] J.K. Norskov, F. Besenbacher, J. Bottiger, B.B. Nielsen, A.A. Pisarev, Interaction of hydrogen with defects in metals – interplay between theory and experiment, Phys. Rev. Lett. 49 (1982) 1420–1423.
[43] Y.L. Liu, Y. Zhang, H.B. Zhou, G.H. Lu, F. Liu, G.N. Luo, Vacancy trapping mechanism for hydrogen bubble formation in metal, Phys. Rev. B 79 (2009) 172103.
[44] X.S. Kong, Y.W. You, X.Y. Li, X.B. Wu, C.S. Liu, J.L. Chen, G.N. Luo, Towards understanding the differences in irradiation effects of He, Ne and Ar plasma by investigating the physical origin of their clustering in tungsten, Nucl. Fusion 56 (2016) 106002.